

# Optical properties of alumina titanium carbide sliders used in rigid disk drives

Peter de Groot

A common material for read-write sliders is a composite of alumina ( $\text{Al}_2\text{O}_3$ ) and titanium carbide (TiC), with a grain size of the order of  $1\ \mu\text{m}$ . I derive the effective complex reflectivity of this material, using scalar diffraction theory and the known indices of refraction of  $\text{Al}_2\text{O}_3$  and TiC. The effective reflectivity is a function of the relative surface area of the exposed TiC grains as well as of the numerical aperture of the collection optics. The theory resolves several known discrepancies between ellipsometry and reflectometry of  $\text{Al}_2\text{O}_3$ -TiC. The theory also predicts a systematic error in the phase shift on reflection calculation. These results are of considerable interest for surface shape metrology of the slider as well as for optical flying-height testing and control of pole-tip recession. © 1998 Optical Society of America  
OCIS codes: 120.3180, 120.2130, 120.2830, 120.4530, 120.4640, 120.5410.

## 1. Introduction

High-precision metrology of the read-write sliders is of critical importance in the manufacture of components for rigid disk drives. Measurements of sliders for pole-tip recession, air-bearing surface (ABS) profile, and dynamic flying height all depend on accurate interferometric analysis. These measurements make assumptions about the optical properties of the materials that make up the ABS.

The most common material for the ABS is a composite of alumina ( $\text{Al}_2\text{O}_3$ ) and titanium carbide (TiC). Under an optical microscope the polished ABS shows grains of brightly reflecting TiC embedded in alumina (Fig. 1). Despite the complexity of the surface, the common practice in interferometric metrology is to equate  $\text{Al}_2\text{O}_3$ -TiC with a smooth homogeneous material. One can then calculate the reflectivity by using the real and the imaginary parts  $n$  and  $k$ , respectively, of an effective index of refraction. According to this point of view, the effective  $n$  and  $k$  measured by an ellipsometer are sufficient to describe the optical properties of  $\text{Al}_2\text{O}_3$ -TiC composites, including any material-dependent phase change on reflection (PCOR).<sup>1</sup>

A possible physical justification for the  $n$  and  $k$

model for  $\text{Al}_2\text{O}_3$ -TiC is effective-medium (EM) theory, which seeks to ascribe to a rough, composite surface structure an effective dielectric permeability.<sup>2</sup> The EM theory has been successful in describing the optical properties of certain fine-grain metal-dielectric composites such as Co- $\text{Al}_2\text{O}_3$  Cermets.<sup>3</sup> Unfortunately, the surface structure of  $\text{Al}_2\text{O}_3$ -TiC is inconsistent with the fundamental assumptions behind EM theory, which is valid for grain sizes far below the wavelength of light. From Fig. 1 it is clear that the TiC grains are typically several micrometers in extent and separation. Thus the EM theory cannot be used to justify the  $n$  and  $k$  model for  $\text{Al}_2\text{O}_3$ -TiC.

A possible empirical justification for the  $n$  and  $k$  model is the weak dependence of the predicted PCOR on incident angle in a standard ellipsometer. Because  $n$  and  $k$  are intrinsic material properties, they should be independent of the incident angle in the measurement system. Lacey *et al.*<sup>4</sup> have shown that the ellipsometric  $n$  and  $k$  for incident angles from  $25^\circ$  to  $75^\circ$  provide self-consistent PCOR predictions to within  $\pm 6$  mrad. However, the same data, which appear as Table 1 of Ref. 4, show that  $n$  does in fact vary by 0.13 in an almost linear fashion from  $25^\circ$  to  $75^\circ$ . This variation is inconsistent with the  $n$ -and- $k$  model and is in fact a reason to suspect that the model is not correct.

Another possible empirical justification for the  $n$ -and- $k$  model is the generally good success in obtaining flying-height data from optical testers that rely on  $n$  and  $k$ . The fact that most disk drives do not crash is indirect evidence that there is some utility to using  $n$  and  $k$ . However, given the 2-nm rms surface

The author is with the Zygo Corporation, Laurel Brook Road, Middlefield, Connecticut 06455 (email, peterd@zygo.com).

Received 3 April 1998; revised manuscript received 10 June 1998.

0003-6935/98/286654-10\$15.00/0

© 1998 Optical Society of America

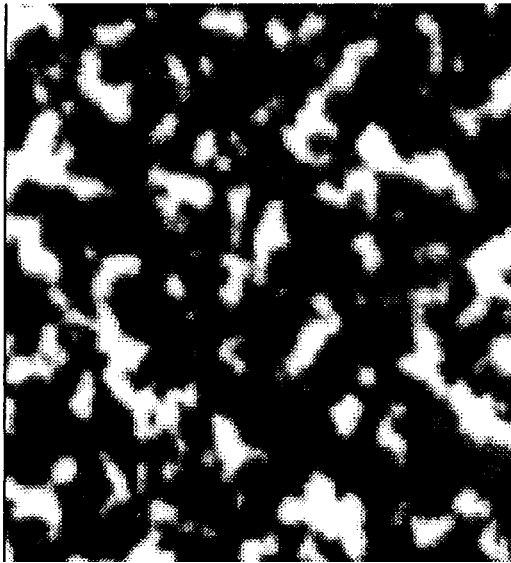


Fig. 1. Microscope image of a polished  $\text{Al}_2\text{O}_3$ -TiC surface. The image width is 25  $\mu\text{m}$ .

roughness of  $\text{Al}_2\text{O}_3$ -TiC together with the common practice of adding constant offsets to test equipment, this indirect evidence has a large uncertainty. It is conceivable that systematic errors of several nanometers have been obscured in optical tests of flying height, particularly if these errors tend toward underestimating the size of the gap.

It is plausible therefore that the  $n$ -and- $k$  model for  $\text{Al}_2\text{O}_3$ -TiC is an oversimplification, leading to significant errors when one is calculating the intensity reflectivity and PCOR of read-write sliders. The ellipsometry community is generally skeptical of its applicability to  $\text{Al}_2\text{O}_3$ -TiC materials.<sup>5</sup> Based on experimental evidence, and given the large size of the TiC grains, I propose in this paper that the dominant optical behavior of  $\text{Al}_2\text{O}_3$ -TiC follows from scalar diffraction theory. Diffraction theory provides a formula for the effective complex reflectivity that more accurately describes  $\text{Al}_2\text{O}_3$ -TiC than the traditional  $n$ -and- $k$  model. The same theory provides guidelines as to how best to use and interpret ellipsometric analysis, thereby improving the accuracy of traditional testing procedures that rely on effective  $n$  and  $k$ .

## 2. Ellipsometry and Reflectometry

I begin here with a brief review of polarized light and its interaction with a flat surface in order to introduce notation for the balance of the paper.

For the general case of an interaction of a polarized electric field with matter, we need four parameters to determine the outcome. If the interaction is a surface reflection, then we bundle four parameters into two complex reflectivities  $r_{s,p}$  as follows:

$$E'_{s,p} = r_{s,p} E_{s,p}, \quad (1)$$

where  $E_{s,p}$  and  $E'_{s,p}$  are the electric-field components for the  $s$ - and  $p$ -polarization states, respectively, be-

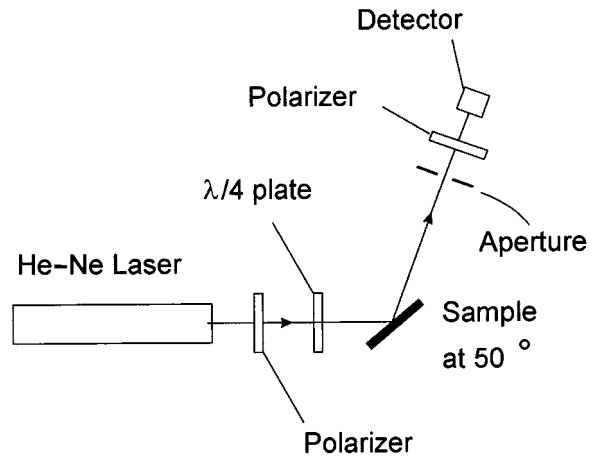


Fig. 2. Null ellipsometer using a 633-nm He-Ne laser.

fore and after they undergo reflection from the surface.

There are important situations for which the number of independent parameters in a surface reflection is fewer than four. The most important is the case of a reflection from a single interface between two homogeneous, isotropic media, referred to in ellipsometry as the two-phase model.<sup>6</sup> For this special case the reflection coefficients can be calculated for any angle of incidence by use of the Fresnel formulas<sup>7</sup> and the complex index of refraction, often written as

$$v = n + ik. \quad (2)$$

The four parameters incorporated into the complex reflectivities  $r_{s,p}$  reduce for this special case to the two real parameters  $n$  and  $k$ .

Because there are only two optical parameters, it is possible to characterize the reflecting properties of a homogeneous material completely from only two measurements. In ellipsometry these two measurements are the square root of the ratio of the  $s$ - and  $p$ -polarization intensity reflectivities  $R_{s,p} = |r_{s,p}|^2$ , expressed as the tangent of an angle  $\Psi$ , and the difference  $\Delta$  between the phase angles  $\arg(r_{s,p})$ . It is well understood, however, that just because we can calculate  $n$  and  $k$  from the ellipsometric  $\Delta$  and  $\Psi$  it does not necessarily follow that the sample material actually has a single complex index  $v$  from which we can calculate the complex reflectivities  $r_{s,p}$  for all angles of incidence.

To examine the appropriateness of using a single complex index for  $\text{Al}_2\text{O}_3$ -TiC, I performed ellipsometry and reflectometry experiments on four different uncoated samples, using the small-aperture, two-zone null ellipsometer shown in Fig. 2.<sup>8</sup> I measured  $n$  and  $k$  at an incident angle of  $50^\circ$  and then measured the intensity reflectivity  $R_s$  at  $50^\circ$  and  $R_0$  at normal incidence. In every case the measured intensity reflectivity was  $\sim 20\%$  lower than the predicted value based on the  $n$ -and- $k$  model. The surface roughness of  $\text{Al}_2\text{O}_3$ -TiC is not large enough to explain such a large intensity loss.

### 3. Scalar Diffraction Model

We can make a few good guesses as to what actually happens when light reflects from an  $\text{Al}_2\text{O}_3$ -TiC surface. An incident electric field  $E_0$  upon a large-grain composite (i.e., grain size  $>$  wavelength) sees two distinct materials. Some portions of the field reflect from the TiC grains, whereas other portions reflect from the  $\text{Al}_2\text{O}_3$ . The discontinuous surface features scatter or diffract light into a broad range of angles, with a resultant amplitude and phase that depend on the size and distribution of the TiC. The imaging optics of an ellipsometer, a flying-height tester, or a low-magnification microscope are normally arranged to collect light at the specular reflection angle. The low numerical aperture (N.A.) of the imaging optics filters out the information about grain size and location, resulting in a coherent superposition of the fields reflected from the TiC and the  $\text{Al}_2\text{O}_3$ . However, much of the diffracted light falls outside the aperture of the optics and is lost.

This picture underscores the importance of diffraction theory in any theoretical model of the optical properties of  $\text{Al}_2\text{O}_3$ -TiC. Consequently, I will develop in this section a simple scalar diffraction (SD) model for  $\text{Al}_2\text{O}_3$ -TiC as an alternative to the more familiar  $n$ -and- $k$  model. I should emphasize here that I make no claim as to the novelty or generality of this model, which is not meant to be a significant contribution of the development of diffraction theory. Rather, the purpose here is to emphasize the importance of treating  $\text{Al}_2\text{O}_3$ -TiC as a heterogeneous material when one is interpreting the results of interferometric measurements.

To make things simple, I use the Fraunhofer approximation, which makes it possible to predict the electric-field pattern far from the surface by using the Fourier transform of the aperture function of the surface. The aperture function is a two-dimensional description of the surface that comprises the various surface pieces according to their size, position, and complex reflectivity. One approach to defining the aperture function would be to map the surface by use of a combination of microscope and scanning probe data. That is not the approach that I take here. Instead, I examine a specific and convenient surface structure that is relatively easy to transform analytically. The hypothesis, which will not be proved rigorously, is that this simplified model has all the important characteristics of the more general and chaotic surface structure of  $\text{Al}_2\text{O}_3$ -TiC.

Figure 3 shows a model in which the TiC is arranged into stripes that have a period  $D$  and a width  $\epsilon D$ . The TiC therefore makes up a proportion  $\epsilon$  of the exposed surface area, and the rest is  $\text{Al}_2\text{O}_3$ . In this idealization there are no discontinuous features in the  $y$  direction, so only the  $x$  direction is relevant to the diffraction problem. As a further simplification, the surface and the incident illumination are presumed to be of infinite extent in both the  $x$  and the  $y$

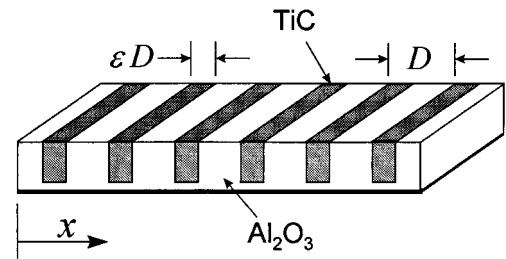


Fig. 3. Simple model of composite  $\text{Al}_2\text{O}_3$ -TiC that comprises stripes of TiC embedded in  $\text{Al}_2\text{O}_3$ .

directions. We now write the full aperture function as

$$A = r_A + \Delta r A_G, \quad (3)$$

where

$$A_G = \text{comb}(x/D) \otimes \text{rect}(x/\epsilon D), \quad (4)$$

$r_A$  is the complex reflectivity of the  $\text{Al}_2\text{O}_3$ , and  $\Delta r = (r_T - r_A)$  is the difference in complex reflectivity between the TiC and the  $\text{Al}_2\text{O}_3$ . The comb and rect functions will be recognized as standard functions from Goodman's book on Fourier optics<sup>9</sup>:

$$\text{comb}(a) = \sum_{m=-\infty}^{\infty} \delta(a - m), \quad (5)$$

$$\text{rect}(a) = \begin{cases} 1 & |a| \leq 1/2 \\ 0 & |a| > 1/2 \end{cases} \quad (6)$$

where  $\delta$  is the Dirac delta function.

Light impinging upon the sample diffracts into a far-field pattern given by the Fourier transform  $U$  of the aperture function  $A$ , which for the model surface involves a single integral over  $x$ . The transform of the aperture is

$$U = r_A \delta(f) + \epsilon \Delta r \text{comb}(Df/\lambda) \frac{\sin(\pi \epsilon Df/\lambda)}{\pi \epsilon Df/\lambda}. \quad (7)$$

Here  $f$  is the differences of the sines of the incident and diffraction angles. The reflected light includes a series of diffracted beams generated by the discontinuous structure of the surface, modulated by a sinc function.

Real  $\text{Al}_2\text{O}_3$ -TiC sliders' surfaces do not have a simple grating structure. The TiC grains are of random size, shape, and separation. Experimentally, the diffraction pattern appears as a bright, well-defined specular reflection surrounded by a halo of scattered light. One can imagine that this halo is built up from the superposition of many grating patterns, corresponding to the diffracted light from various spatial frequency components of the surface structure. Keeping this picture in mind, it is plausible that many of the more important optical characteristics of the true surface structure are contained in the simplified model shown in Fig. 3.

#### 4. Effective Reflectivity

From Eq. (7) and from experimental observation of actual reflected-light patterns it is clear that the apparent optical properties of Al<sub>2</sub>O<sub>3</sub>-TiC will be a function of the N.A. of the collection optics. As it turns out, it is possible to define an effective complex reflectivity  $\tilde{r}$  only for a system that has a low N.A.

In most ellipsometers the collection optics have a N.A. of less than 0.05 and capture only the central,  $m = 0$ , beam. The other beams are diffracted outside the aperture of the optics. The effective complex reflectivity  $\tilde{r}$  for this case is

$$\tilde{r} = r_A + \varepsilon(r_T - r_A). \quad (8)$$

The intensity reflectivity and PCOR for low-N.A. systems are then

$$\tilde{R} = |\tilde{r}|^2, \quad (9)$$

$$\tilde{\alpha} = \arctan \left[ \frac{\text{Im}(\tilde{r})}{\text{Re}(\tilde{r})} \right]. \quad (10)$$

The symbol  $\sim$  is meant to distinguish the SD results from those derived from the effective  $n$  and  $k$ . Although the notation does not show it explicitly, the effective complex reflectivity  $\tilde{r}$  is of course a function of the polarization state and the incident angle.

Continuing with this low-N.A. calculation, suppose that we are using Al<sub>2</sub>O<sub>3</sub>-TiC in a two-beam interferometer, with the reference surface having a complex reflectivity  $r_{\text{ref}}$ . If we neglect any common coefficients, the interference intensity is

$$\tilde{I} = |r_{\text{ref}} \exp(i\theta) + \tilde{r}|^2, \quad (11)$$

where  $\theta$  is the phase delay attributable to the optical path difference in the interferometer. The interference intensity works out to be

$$\tilde{I} = R_{\text{ref}} + \tilde{R} + 2\sqrt{R_{\text{ref}}\tilde{R}} \cos(\theta - \alpha_{\text{ref}} - \tilde{\alpha}), \quad (12)$$

where  $R_{\text{ref}}$  is the square magnitude of  $r_{\text{ref}}$  and  $\alpha_{\text{ref}}$  is the PCOR for the reference surface. This is just what one would expect from an interferometry experiment with a homogeneous material that has a true complex reflectivity  $\tilde{r}$ . Thus, even though the value of  $\tilde{r}$  cannot be derived from a single complex index of refraction, the concept of an effective complex reflectivity is valid.

The high-N.A. situation is more complicated. A high-N.A. optical system captures light from various diffraction orders and is capable of producing images of the individual grains of TiC in a slider ABS. If an electronic camera resolves the imaged grains, then the TiC and the Al<sub>2</sub>O<sub>3</sub> must be treated as separate materials. If a single, large-area detector measures the total intensity, then the effective-surface result is the integrated sum of the intensity from each surface component. Assuming that we are dealing with a

large-area detector, the high-N.A. intensity reflectivity  $\hat{R}$  is

$$\hat{R} = R_A + \varepsilon(R_T - R_A). \quad (13)$$

The high-N.A. intensity reflectivity  $\hat{R}$  is always greater than or equal to the low-N.A. intensity reflectivity  $\tilde{R}$ :

$$\hat{R} - \tilde{R} = \varepsilon(1 - \varepsilon)|r_T - r_A|^2. \quad (14)$$

As one might expect, the high-N.A. optics gather more light and see a brighter surface than the low-N.A. optics. The  $\hat{R}$  value is the apparent intensity reflectivity that one would measure in a simple reflectometry experiment with a large collection aperture.

Importantly, although we can define an apparent intensity reflectivity  $\hat{R}$  for an effective surface viewed by high-N.A. optics, it is not possible to define a single, complex reflectivity that is valid for all types of measurement. For example, in a high-N.A. two-beam interferometer the measured intensity is the incoherent addition of interference effects for the two materials taken separately. The resultant interference function  $\hat{I}$  is

$$\hat{I} = R_{\text{ref}} + \hat{R} + 2\sqrt{R_{\text{ref}}\hat{R}} \cos(\theta - \alpha_{\text{ref}} - \tilde{\alpha}). \quad (15)$$

The interference phase dependence  $\theta - \alpha_{\text{ref}} - \tilde{\alpha}$  and the modulation amplitude  $2\sqrt{R_{\text{ref}}\tilde{R}}$  are the same as for the low-N.A. situation, but there is an intensity offset  $\hat{R} - \tilde{R}$  that reduces fringe contrast even in an idealized system. The need for two intensity reflectivities  $\hat{R}$  and  $\tilde{R}$  to describe the optical behavior of the same surface is inconsistent with the concept of an effective complex reflectivity.

To conclude this section, it is possible to define an effective complex reflectivity  $\tilde{r}$  for composite Al<sub>2</sub>O<sub>3</sub>-TiC, provided that the N.A. of the optical system is small. The effective complex reflectivity  $\tilde{r}$  is equal to the weighted sum of the complex reflectivities  $r_{A,T}$  for Al<sub>2</sub>O<sub>3</sub> and TiC.

#### 5. Reflectometry and Ellipsometry Experiments

The SD model provides a means for calculating an effective complex reflectivity  $\tilde{r}$  of Al<sub>2</sub>O<sub>3</sub>-TiC as a function of polarization state, incident angle, and apparent surface composition  $\varepsilon$  of TiC. There are a variety of experimental means for verifying the theory directly.

First, it should be possible to predict the  $n$  and  $k$  that would be measured by an ellipsometer, even though for the moment the usefulness of these apparent  $n$  and  $k$  values is in doubt. Equation (8) provides the effective complex reflectivity  $\tilde{r}$  for the  $s$ - and  $p$ -polarization states, from which it is possible to predict the ellipsometric  $\Delta$  and  $\Psi$  from Eqs. (9) and (10). For this calculation the assumed refractive indices of Al<sub>2</sub>O<sub>3</sub> and TiC are  $1.7 + 0i$  and  $3.5 + 2.5i$ , respectively. From Fig. 4 and Table 1 it appears that suitable values for  $\varepsilon$  are 20% to 35%. Table 2 provides a

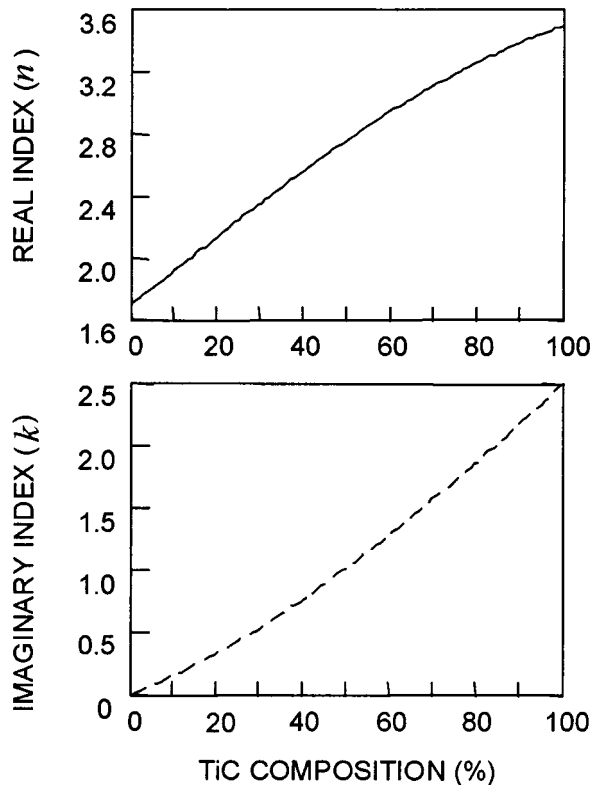


Fig. 4. Predicted effective  $n$  and  $k$  values as a function of the TiC composition  $\epsilon$ , according to the SD model in the low-N.A. limit.

direct comparison with the four samples in Table 1. After  $\epsilon$  is optimized for each sample, the average difference between theoretical and experimental  $n$  and  $k$  values is less than 0.03. The ability to predict the two values  $n$  and  $k$  by use of only one parameter  $\epsilon$  is an important validation of the theory.

The SD model also predicts a variation of the effective  $n$  and  $k$  as measured by an ellipsometer at different incident angles. This is quite different behavior from that of truly homogeneous materials, for which  $n$  and  $k$  do not change with angle. It will be recalled from Section 1 that Lacey *et al.* reported measurements of  $n$  and  $k$  over a range of incident angles and that these results showed a small but measurable angle dependence.<sup>4</sup> Figure 5 shows

Table 1. Normal-Incidence Intensity Reflectivity  $R_0$  and 50° s-Polarization Intensity Reflectivity  $R_s$  for Four  $\text{Al}_2\text{O}_3$ -TiC Samples

Sample Number	Index $v$	Measured Reflectivity	$n$ -and- $k$ Model Prediction	Error (%)
1	2.16 + 0.40i	$R_s = 0.242$	0.286	16
		$R_0 = 0.122$	0.148	18
2	2.22 + 0.43i	$R_s = 0.242$	0.298	19
		$R_0 = 0.127$	0.157	19
3	2.19 + 0.56i	$R_s = 0.248$	0.250	20
		$R_0 = 0.132$	0.132	20
4	2.37 + 0.54i	$R_s = 0.268$	0.334	20
		$R_0 = 0.144$	0.185	22

Table 2. Predicted Optical Constants When Only the TiC Surface Composition  $\epsilon$  is Used as a Variable Parameter

Sample Number	SD Theory			Experiment	
	$\epsilon$ (%)	$n$	$k$	$n$	$k$
1	21.8	2.18	0.38	2.16	0.40
2	24.0	2.23	0.42	2.22	0.43
3	26.2	2.28	0.47	2.19	0.56
4	30.0	2.36	0.55	2.37	0.54

that the predictions of the SD model dependence correlate well with these independent experimental results.

It is also possible to predict and to measure accurately the intensity reflectivity of a sample surface. Figure 6 compares the intensity reflectivities for a TiC surface composition  $\epsilon = 30\%$ . For this figure I first calculated the effective  $n$  and  $k$  values that would be observed in an ellipsometer at 50° for this composition of TiC. I then calculated the intensity reflectivity  $R$  for each polarization state according to the Fresnel equations for these  $n$  and  $k$  and compared them with the results  $\bar{R}$  for the SD theory. The

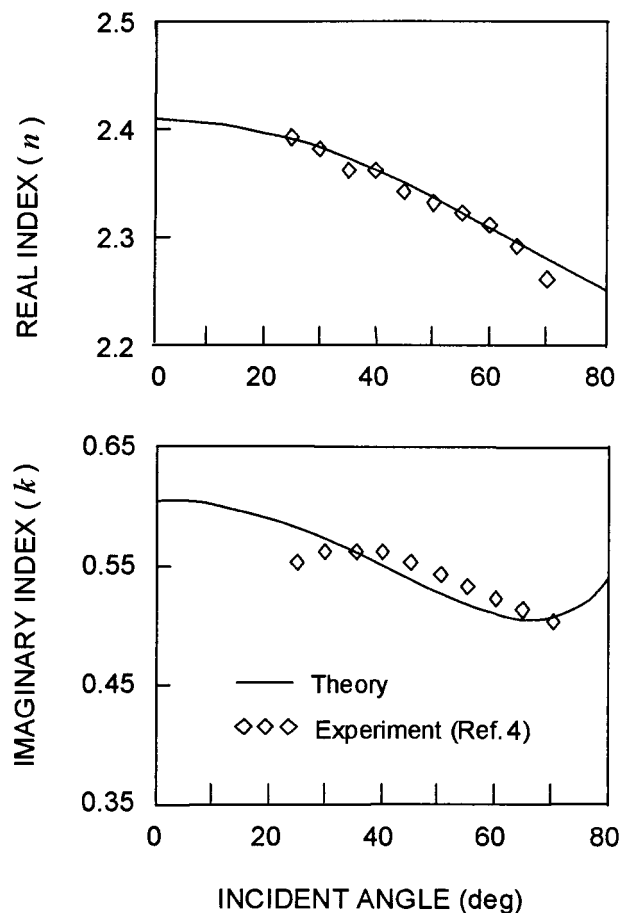


Fig. 5. Comparison of experimental and theoretical variation of measured  $n$  and  $k$  with incident angle for  $\text{Al}_2\text{O}_3$ -TiC. The experimental data are from Ref. 4. For a true homogeneous material,  $n$  and  $k$  would be constant.

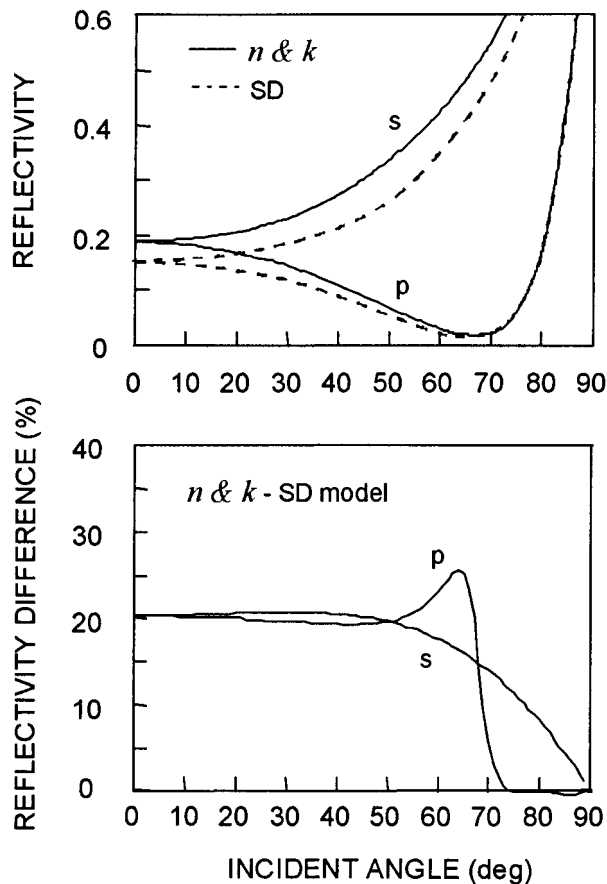


Fig. 6. Comparison of the predicted intensity reflectivities  $R$  for the  $n$ -and- $k$  model and  $R$  for the SD model. The SD model predicts a 20% relative intensity difference at normal incidence, confirming the experimental results in Table 1.

upper graph in Fig. 6 shows that there are significant differences for all incident angles, and the lower graph displays the difference as a relative percentage. The SD model predicts an  $\sim 20\%$  discrepancy over a wide range of incident angles, consistent with the experimental results in Table 1.

## 6. Phase Change on Reflection

The one thing that we cannot measure directly, at least not easily or accurately, is the absolute PCOR. That this is so is unfortunate, because the absolute PCOR has a first-order influence on interferometric metrology. Given the difficulty in directly measuring absolute PCOR, it would be convenient if the predictions of the SD and  $n$  and  $k$  models agreed on at least this one point. They do not. The present theory shows that using the effective  $n$  and  $k$  results in an overestimate of the PCOR.

A PCOR calculation for  $\epsilon = 30\%$  appears in Fig. 7. It is interesting (and a little frustrating) that the large discrepancy between the PCOR predictions of the two models is invisible to ellipsometry. The ellipsometric  $\Delta$  on which the effective  $n$  and  $k$  are based is the difference between the  $s$  and the  $p$  PCOR's, not the absolute value for either polarization. As Fig. 7 indicates, the PCOR discrepancy between the two

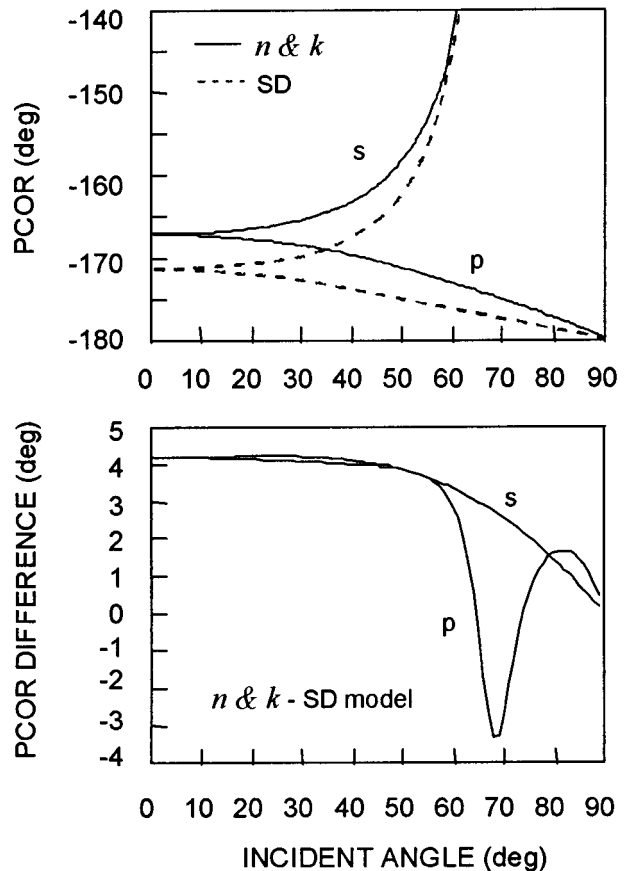


Fig. 7. Theoretical PCOR. The SD model predicts a PCOR at normal incidence that is  $4^\circ$  lower than the value calculated with the effective  $n$  and  $k$ .

models is nearly identical for both polarization states for incident angles from  $0^\circ$  to  $60^\circ$ , and the polarization-dependent variations near  $68^\circ$  are difficult to resolve.

These theoretical PCOR results show that, if we were to characterize a slider ABS by using ellipsometry and subsequently perform interferometric measurements on the same sample by using He-Ne light at normal incidence, the average surface height would be incorrect by 3 nm. For interferometric profile measurements, such an error might go unnoticed. An exception is a profile measurement that involves dissimilar materials, such as in pole-tip recession measurement. At present such measurements require a PCOR calibration that uses a coated witness sample.<sup>10</sup> However, there is considerable interest in calculating the optical properties by means of *in situ* ellipsometry.<sup>11,12</sup> This now appears to be less straightforward than one might hope.

A more immediate problem arises in optical flying-height testing. Optical flying-height testers employ a rotating glass disk in place of the magnetic disk and use the thin-film interference between the slider ABS and the glass to measure the gap.<sup>13,14</sup> Typically, an off-site ellipsometer measures the effective  $n$  and  $k$  at each wavelength on a representative sampling of sliders to correct for the PCOR. An alternative is to

combine the role of the ellipsometer with that of the flying-height tester, by means of a high-speed polarization interferometer working at a 50° angle of incidence.<sup>15,16</sup> No matter how  $n$  and  $k$  are calculated, SD theory predicts that the calculated PCOR will be incorrect by 4°, resulting in an offset in the direction of underestimating the flying height.

The PCOR error raises some interesting questions. There is so much accumulated experience with Al<sub>2</sub>O<sub>3</sub>-TiC that one might expect to have seen such an offset. One possible reason that this has not yet happened is the 2-nm rms surface roughness of polished Al<sub>2</sub>O<sub>3</sub>-TiC. High-resolution surface profiles with an atomic-force microscope show peak-valley roughness of as much as 20 nm on 50-μm<sup>2</sup> areas, with the TiC raised several nanometers on average above the Al<sub>2</sub>O<sub>3</sub>. It is difficult to gain access mechanically to the average surface position, which is the optical point of reference when one is defining PCOR. Mechanical contact measurements will tend therefore to overestimate the PCOR in the same direction and perhaps by the same magnitude as the  $n$  and  $k$  model.

### 7. Repairing the $n$ and $k$ Model

Judging from the results in Sections 5 and 6, the effective  $n$  and  $k$  lead to fairly serious discrepancies, both in the measured PCOR and in the intensity reflectivity. It would be tempting to abandon the concept of effective  $n$  and  $k$  for Al<sub>2</sub>O<sub>3</sub>-TiC. However, doing so would leave the metrologist without a practical means of accommodating material-dependent effects in the optical inspection of sliders.

Suppose that the errors that we have been talking about were constant offsets, to some acceptable degree of approximation. Then  $n$  and  $k$  as measured by an ellipsometer would provide a relative correction, adjusting the measurement parameters to accommodate differences between sliders. If this were the case, we could resolve the discrepancies between the  $n$ -and- $k$  and the SD models by defining the effective complex reflectivity as follows:

$$r' = (1 - \mu)r \exp(i\delta),$$

where  $r$  is the  $n$ -and- $k$  complex reflectivity,  $\mu$  is the square root of the apparent intensity loss, and  $\delta$  is a PCOR offset.

Figure 8 for a 50° angle of incidence shows that a constant offset  $\delta = -3.8^\circ$  brings the PCOR results to within  $\pm 0.4^\circ$  for a TiC composition range of 15% <  $\epsilon$  < 40%. Similarly for the intensity reflectivity, a  $\mu$  of 9.5% brings the predicted intensity reflectivity to within  $\pm 0.01$  over the same range of  $\epsilon$ . At normal incidence, the offsets are somewhat higher ( $\delta_N = 4.2^\circ$  and  $\mu_N = 10\%$ ), but the correlation is just as good. A constant  $\mu$  and  $\delta$  appears to be adequate for tracking changes in the apparent surface composition  $\epsilon$  of TiC.

Another way in which the composite material can change is with the optical properties of the TiC or the Al<sub>2</sub>O<sub>3</sub>. Suppose for example that the real part  $n_T$  of the refractive index of TiC varies from 3.2 to 3.8, depending on variability in processing and composite

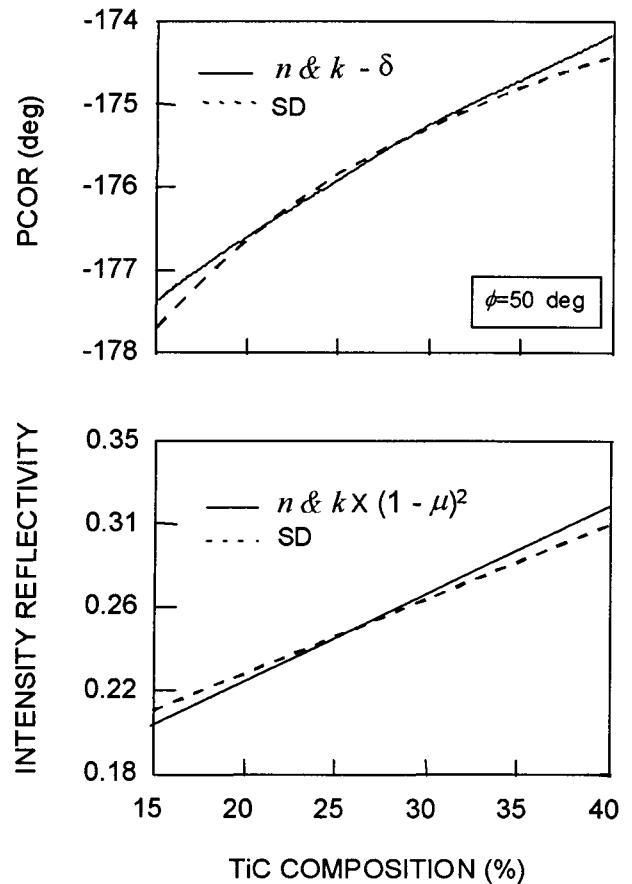


Fig. 8. Theoretical s-polarization PCOR and intensity reflectivity with the constant  $\mu = 9.5\%$  and  $\delta = 3.8^\circ$  offsets, as a function of the TiC composition  $\epsilon$  at an incident angle of 50°. The  $\mu$  and  $\delta$  make it possible to continue to use  $n$  and  $k$  to map changes in Al<sub>2</sub>O<sub>3</sub>-TiC composition.

structure. This change has a negligible effect on the intensity reflectivity but alters the PCOR at normal incidence by 2° of phase. It also alters the effective  $n$  and  $k$  as measured by an ellipsometer, indicating that ellipsometry is a sensitive way to detect such changes. Figure 9 compares the predicted PCOR when the effective  $n$  and  $k$  together with the constants  $\mu_N$  and  $\delta_N$  are used for a normal-incidence interferometry measurement.

Still another way in which the PCOR can change is with a change in relative surface height between the TiC and the Al<sub>2</sub>O<sub>3</sub>. The TiC grains are in fact a few nanometers higher on average than the Al<sub>2</sub>O<sub>3</sub>, which has the effect of introducing a different phase delay between the TiC and the Al<sub>2</sub>O<sub>3</sub>. The net result is similar to changing the index of refraction of the two materials, with the greatest effect on the PCOR. Here again, the use of effective  $n$  and  $k$  provides a means of tracking these changes to reduce the net error.

### 8. Carbon Overcoats

The use of thin-film overcoats has become common to improve the lubrication properties of the slider-disk interface. Most often, the coating is diamondlike

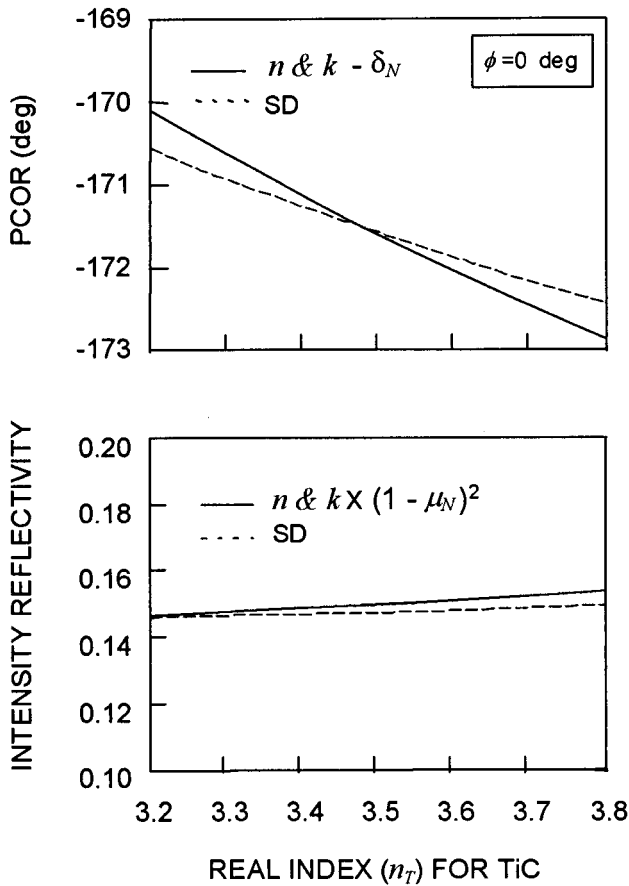


Fig. 9. Theoretical s-polarization PCOR and intensity reflectivity at normal incidence as a function of a variable refractive index for TiC. The  $n$  and  $k$  results include the constant offsets  $\mu_N = 10\%$  and  $\delta_N = 4.2^\circ$ . The TiC composition  $\epsilon$  is fixed at 30%.

carbon (DLC; index,  $2.4 + 0.5i$ ) over an adhesion layer of silicon dioxide ( $\text{SiO}_2$ ; index, 1.46). These coatings have an important effect on the optical properties of the slider. If  $\text{Al}_2\text{O}_3$ -TiC were homogeneous, it would be a straightforward (although not easy) exercise to determine the effective PCOR for coated sliders. Lue *et al.* performed this calculation and concluded that the error that results from applying traditional ellipsometric methods to coated sliders would be negligible.<sup>17</sup>

The results of the SD model are somewhat different. In the SD model the  $\text{Al}_2\text{O}_3$  and the TiC are treated as entirely independent surface features. Coatings are incorporated into two polarization-dependent effective complex reflectivities  $z'_A$  and  $z'_T$ , which replace the bare-surface complex reflectivities  $r_A$  and  $r_T$  in Eq. (8). One way to calculate  $z'_A$  and  $z'_T$  is first to define a function  $\Gamma$ , given by the Drude formula

$$\Gamma(r_1, r_2, \phi', h, v') = \frac{r_1 + r_2 \exp[ikhv' \cos(\phi')]}{1 + r_1 r_2 \exp[ikhv' \cos(\phi')]} \quad (16)$$

The function  $\Gamma$  provides the effective complex reflectivity of two surfaces separated by a medium of thickness  $h$  and index  $v'$ . The surfaces have complex

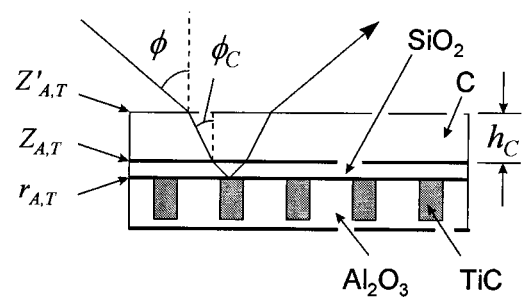


Fig. 10. Simple model of  $\text{Al}_2\text{O}_3$ -TiC with a DLC coating and a  $\text{SiO}_2$  adhesion layer.

reflectivities  $r_1$  and  $r_2$ , and  $\phi'$  is the transmission angle through the medium. A sequence of  $\Gamma$  functions accounts for multiple layers (see Fig. 10). Thus for a DLC coating with a  $\text{SiO}_2$  adhesion layer we have

$$z'_{A,T} = \Gamma(r_C, z_{A,T}, \phi_C, h_C, v_C) \quad (17)$$

where

$$z_{A,T} = \Gamma(r_S, r_{A,T}, \phi_S, h_S, v_S) \quad (18)$$

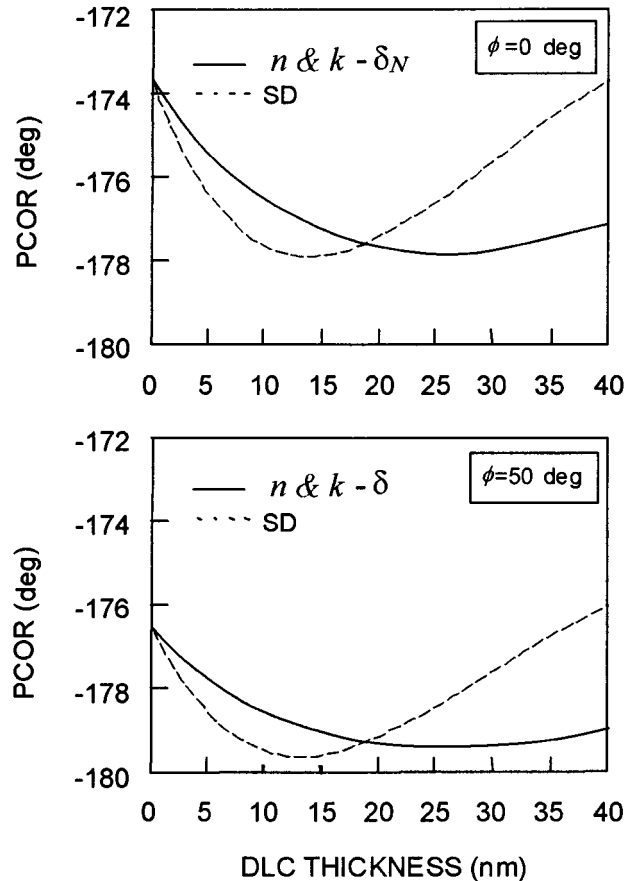


Fig. 11. PCOR at normal incidence and at an incident angle  $\phi$  of  $50^\circ$  for the  $n$ -and- $k$  and the SD models, for variable DLC thickness. For a fixed relative TiC composition,  $\epsilon = 20\%$ . The ellipsometry for  $n$  and  $k$  in both cases is calculated at  $50^\circ$ . The  $n$ -and- $k$  model prediction includes the offsets  $\delta = -3.8^\circ$  and  $\delta_N = -4.2^\circ$ .

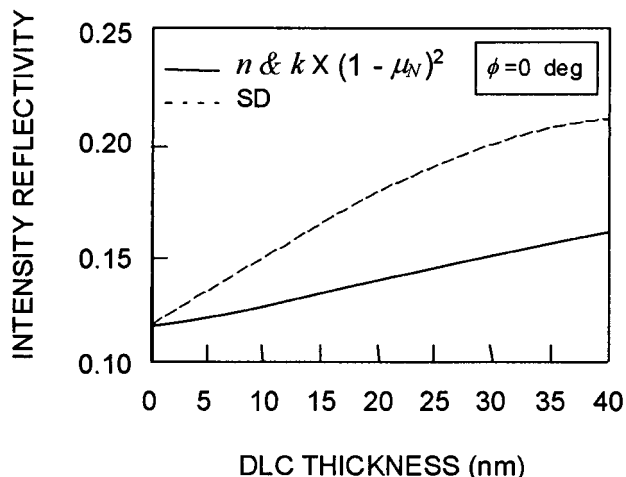


Fig. 12. Intensity reflectivity at normal incidence for variable DLC thickness for a nominal scatter-loss coefficient  $\mu_N = 10\%$ . The ellipsometry for  $n$  and  $k$  is calculated at a  $50^\circ$  incident angle, and the TiC composition is  $\epsilon = 20\%$ . The large divergence forces a reduction of the  $\mu_N$  factor from 10% to a compromise value of 5%.

for

$$\sin(\phi_C) = \frac{\sin(\phi)}{v_C}, \quad (19)$$

$$\sin(\phi_S) = \frac{\sin(\phi)}{v_S}. \quad (20)$$

The complex reflectivities for the air–DLC and DLC– $\text{SiO}_2$  interfaces, denoted  $r_C$  and  $r_S$ , respectively, are calculated from the Fresnel formulas.

The results in Fig. 11 show that a constant PCOR offset  $\delta$  brings the PCOR prediction close enough to the SD model prediction to justify using  $n$  and  $k$  as an approximate correction with DLC coatings. The residual error is larger than that predicted by Lue *et al.*<sup>17</sup> but is nonetheless constrained to  $\pm 1^\circ$  up to a 25-nm coating thickness for both normal incidence and  $50^\circ$ . A more difficult problem is the intensity reflectivity, which relates to the  $\mu$  factor. Figure 12 shows that the intensity reflectivity changes rather dramatically as the DLC coating thickness increases. Consequently, the optimum value of  $\mu$  decreases with coating thickness.<sup>18</sup> Recall that the  $\mu$  factor is approximately equal to half of the intensity reflectivity difference; it would appear that a better value for  $\mu$  at 6-nm DLC thickness would be  $\mu' = 5\%$ . This is what

Table 3. Predicted Intensity Reflectivities and Effective Optical Constants of an  $\text{Al}_2\text{O}_3$ -TiC Sample Known to Have 6 nm of DLC over a 2-nm  $\text{SiO}_2$  Adhesion Layer

Parameter	Experiment	<i>n</i> -and- <i>k</i> Model	SD Model ( $\epsilon = 18.3\%$ )
$n$	2.09	—	2.17
$k$	0.34	—	0.28
$R_s$	0.242	0.270	0.249
$R_0$	0.122	0.136	0.127

Table 4. Observed TiC Surface Composition When Conventional Microscopy is Used Compared with the  $\epsilon$  Found by Optimizing for Best Match to the Effective  $n$  and  $k$

Sample Number	Observed TiC (%)	Optimized $\epsilon$
1	$22.8 \pm 2$	21.8
2	27.6	24.0
3	26.1	26.2
4	28.1	30.0

I observed experimentally for an  $\text{Al}_2\text{O}_3$ -TiC sample known to have a DLC coating (Table 3). If the DLC coating thickness is unknown, it appears most reasonable to chose a compromise value of  $\mu' = 5\%$  as the default.

### 9. Independent Measurement of Surface Composition

The SD model has a single adjustable parameter  $\epsilon$ , which is the relative exposed surface area of TiC. This ought to be something that one could measure independently, for example, by microscopy. The picture in Fig. 1 shows that the TiC grains are significantly brighter than the surrounding  $\text{Al}_2\text{O}_3$ . By sectioning the image according to brightness, it should be possible to estimate the  $\epsilon$  independently of the SD theory.

It turns out that an independent microscope measurement is more subjective than would be desirable, because the intensity distribution is not binary. There are shades of gray around each TiC grain, and it is difficult to establish an objective cutoff level for counting statistics. Nonetheless, I reproduce as Table 4 the results of such a brightness-based analysis, in comparison with the  $\epsilon$  values previously established to optimize agreement between the SD model and ellipsometric tests. The agreement is satisfactory in that the magnitude and the relative ranking of the materials are in reasonable agreement. In particular, there is a clear confirmation that sample 1 has a much smaller exposed TiC grain area than sample 4, leading to lower values of  $n$  and  $k$ .

### 10. Summary and Conclusions

The existing paradigm for approximating the optical properties of  $\text{Al}_2\text{O}_3$ -TiC is to substitute an effective homogeneous medium for the true composite structure. The effective  $n$  and  $k$  of this medium are traditionally presumed to be adequate for the accurate calculation of derived quantities, such as intensity reflectivity and phase change on reflection.

In reality, because of the large grain size of  $\text{Al}_2\text{O}_3$ -TiC, the optical properties of this material are dominated by diffraction. Scalar diffraction theory applied to a simplified surface structure provides much better estimates of reflectivity. If we accept the scalar diffraction model as accurate, there are some important consequences. The intensity reflectivity in low-N.A. systems is 20% lower for uncoated

$\text{Al}_2\text{O}_3\text{-TiC}$  than the  $n$  and  $k$  prediction. In large-N.A. systems the optical behavior of this material is such that it is not possible even to define a self-consistent effective complex reflectivity. Further, the apparent PCOR for  $\text{Al}_2\text{O}_3\text{-TiC}$  for all optical systems will be several degrees of phase smaller than the predicted value for the  $n$ -and- $k$  model.

Despite these discrepancies, it is still possible to use ellipsometry to characterize  $\text{Al}_2\text{O}_3\text{-TiC}$ , provided that we include constant offsets  $\mu$  and  $\delta$  for the intensity and the PCOR, respectively. With these two corrections,  $n$  and  $k$  measured ellipsometrically provide a means of tracking PCOR variations related to changes in composition, refractive index of the constituent materials, surface texture, and DLC coating thickness.<sup>19</sup>

I thank Gregg Gallatin for his careful review of this research and his many helpful suggestions. K. L. Babcock of Digital Instruments Corporation, Santa Barbara, Calif., and G. P. Bernhard, University of Maine, Orono, Maine, performed scanning-probe microscopy analysis of  $\text{Al}_2\text{O}_3\text{-TiC}$  samples that were extremely useful in this study.

#### References and Notes

1. F. Muranushi, K. Tanaka, and Y. Takeuchi, "Estimation of zero-spacing error due to a phase shift of reflected light in measuring a magnetic head slider's flying height by light interference" *Adv. Inf. Storage Syst.* **4**, 371-379 (1992); The same paper was presented at the American Society of Mechanical Engineers Winter Annual Meeting, Atlanta, Ga., 1991.
2. D. M. Wood and N. W. Ashcroft, "Effective medium theory of optical properties of small particle composites," *Phil Mag.* **35**, 269-280 (1977).
3. G. A. Niklasson, C. G. Granqvist, and O. Hunderi, "Effective medium models for the optical properties of inhomogeneous materials," *Appl. Opt.* **20**, 26-30 (1981).
4. C. Lacey, C. Durán, K. Womack, and R. Simmons, "Optical measurement of flying height," in *Proceedings of the Future Dimensions in Storage Symposium* (International Disk Drive Equipment and Materials Association, Santa Clara, Calif., 1997), pp. 81-88.
5. R. Synowicki, "Difficulties associated with analysis of composite head structures using ellipsometry," applications note (J. A. Woollam Company, Lincoln, Neb., 1997).
6. R. M. A. Azzam, "Ellipsometry," in *Handbook of Optics*, M. Bass, ed. (McGraw-Hill, New York, 1995), Vol. 2, Chap. 27, p. 275.
7. M. Born and E. Wolf, *Principles of Optics*, 6th ed. (Pergamon, Oxford, 1987), p. 40.
8. H. G. Tompkins, *A User's Guide to Ellipsometry* (Academic, Boston, Mass., 1993), p. 28.
9. J. W. Goodman, *Introduction to Fourier Optics* (McGraw-Hill, New York, 1968), p. 14.
10. R. Smythe, L. Selberg, and L. Deck, "Pole tip recession measurements of transducers on thin film sliders for rigid disk drives," in *Proceedings of the International Disk Conference in Tokyo, Japan* (International Disk Drive Equipment and Materials Association, Santa Clara, Calif., 1992).
11. E. W. Rogala and H. H. Barrett, "Phase-shifting interferometer/ellipsometer capable of measuring the complex index of refraction and the surface profile of a test surface," *J. Opt. Soc. Am. A* **15**, 538-548 (1998).
12. G. D. Feke, D. P. Snow, R. D. Grober, P. J. de Groot, and L. Deck, "Interferometric back focal plane microellipsometry," *Appl. Opt.* **37**, 1796-1802 (1998).
13. W. Stone, "A proposed method for solving some problems in lubrication," *Commonw. Eng.* **1921**, 115-122.
14. J. M. Fleischer and C. Lin, "Infrared laser interferometer for measuring air-bearing separation," *IBM J. Res. Devel.* **18**, 529-533 (1974).
15. P. de Groot, L. Deck, J. Soobitsky, and J. Biegen, "Polarization interferometer for measuring the flying height of magnetic read-write heads," *Opt. Lett.* **21**, 441-443 (1996).
16. P. de Groot, "Optical gap measuring apparatus and method," U.S. patent 5,557,399 (17 September 1996).
17. K. Lue, C. Lacey, and F. E. Talke, "Measurement of flying height with carbon overcoated sliders," *IEEE Trans. Magn.* **30**, 4167-4169 (1994).
18. Carbon overcoats are crystalline thin films that have a columnar microstructure that can cause significant optical scatter. This additional light loss can be accommodated by an empirical measurement of the scatter-loss coefficient  $\mu$ .
19. An alternative approach is to correlate the reflectance of the slider to the index of refraction by using an empirically derived equation. See K. H. Womack and A. Butler, "Determining the complex refractive index phase offset in interferometric flying height testing," U.S. patent 5,781,299 (14 July 1998).